

**Porous nitrogen-doped carbon-immobilized bimetallic nanoparticles
as highly efficient catalysts for hydrogen generation from hydrolysis
of ammonia borane**

Lingling Guo, Xiaojun Gu,* Kai Kang, Yanyan Wu, Jia Cheng, Penglong Liu,
Haiquan Su*

Inner Mongolia Key Laboratory of Coal Chemistry, School of Chemistry and
Chemical Engineering, Inner Mongolia University, Hohhot 010021, Inner Mongolia,
China

E-mail addresses: xiaojun.gu@yahoo.com; haiquansu@yahoo.com

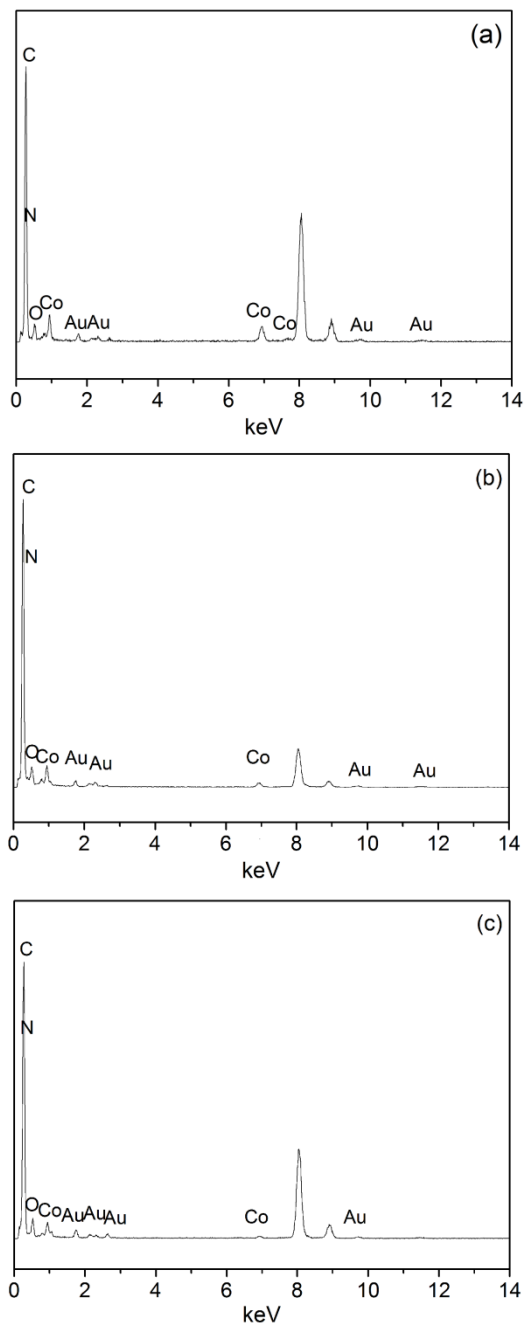


Fig. S1 EDS of (a) AuCo/NXC-1, (b) AuCo/NXC-2 and (c) AuCo/NXC-3 ($\text{Au}/\text{Co} = 1/7$).

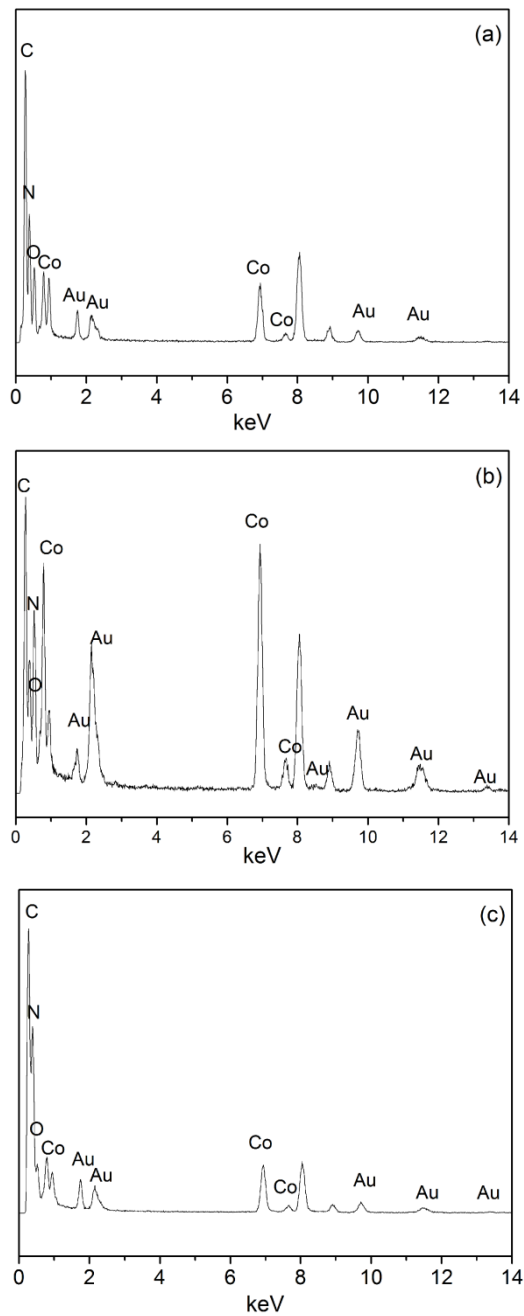


Fig. S2 EDS of (a) AuCo/C₃N₄-1, (b) AuCo/C₃N₄-2 and (c) AuCo/C₃N₄-3 (Au/Co = 1/7).

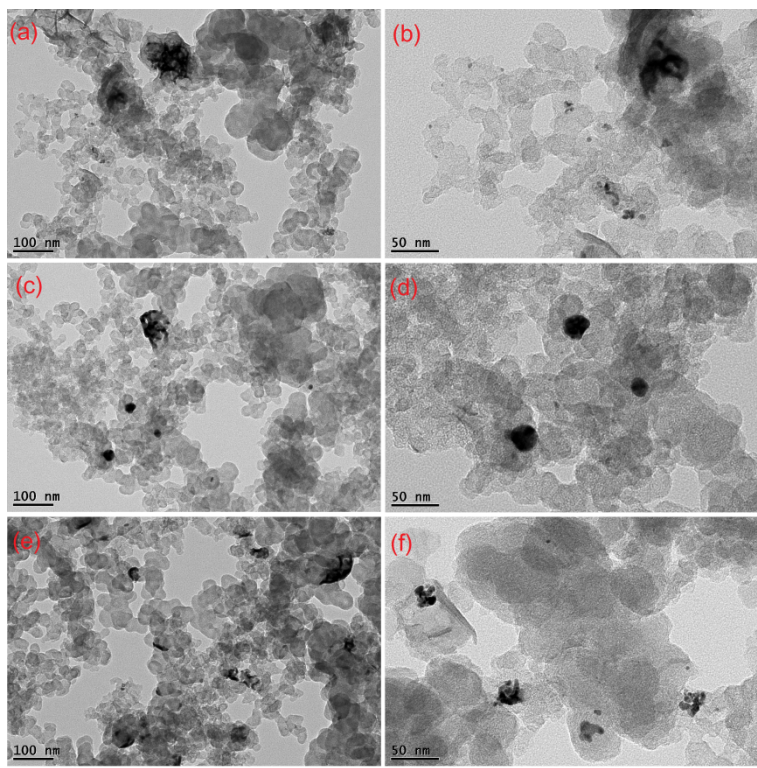


Fig. S3 Representative TEM images of (a, b) AuCo/XC-1, (c, d) AuCo/XC-2 and (e, f) AuCo/XC-3 (Au/Co = 1/7).

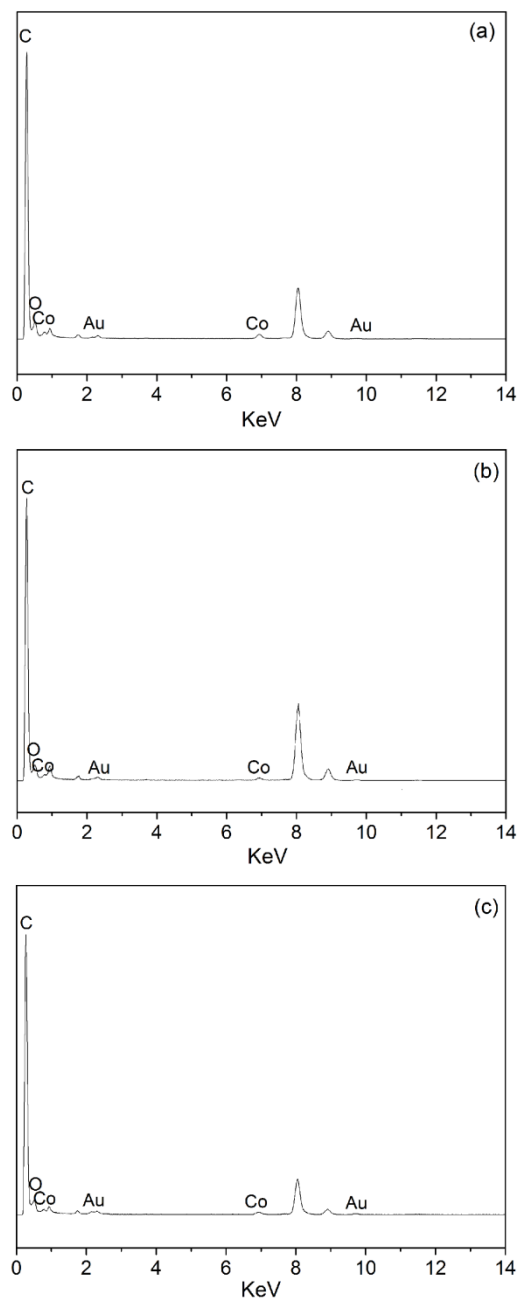


Fig. S4 EDS of (a) AuCo/XC-1, (b) AuCo/XC-2 and (c) AuCo/XC-3 (Au/Co = 1/7).

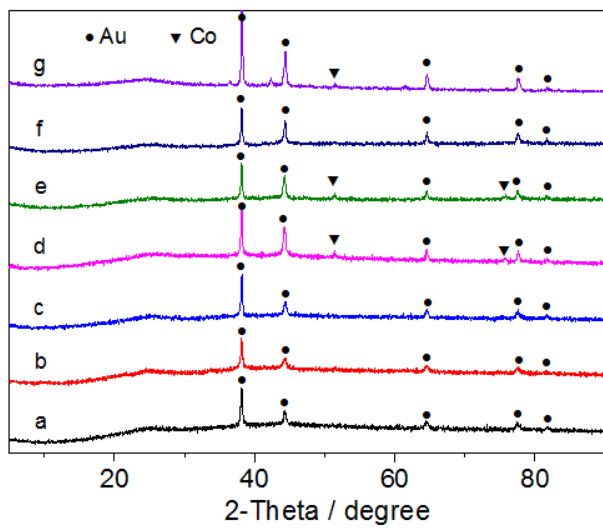


Fig. S5 XRD patterns of (a) AuCo/NXC-1, (b) AuCo/NXC-2 and (c) AuCo/NXC-3; (d) AuCo/NXC-1, (e) AuCo/NXC-2 and (f) AuCo/NXC-3 after heat treatment at 873 K for 4 h in Ar atmosphere; (g) AuCo/NXC-3 after heat treatment at 1173 K for 4 h in Ar atmosphere.

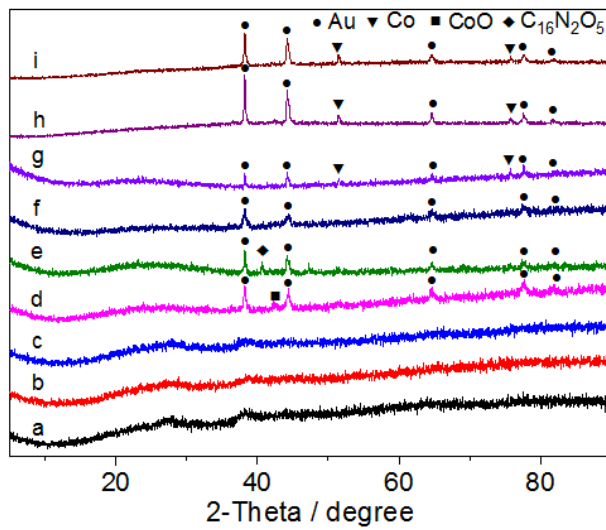


Fig. S6 XRD patterns of (a) AuCo/C₃N₄-1, (b) AuCo/C₃N₄-2 and (c) AuCo/C₃N₄-3; (d) AuCo/C₃N₄-1, (e) AuCo/C₃N₄-2 and (f) AuCo/C₃N₄-3 after heat treatment at 873 K for 4 h in Ar atmosphere; (g) AuCo/C₃N₄-1, (h) AuCo/C₃N₄-2 and (i) AuCo/C₃N₄-3 after heat treatment at 1173 K for 4 h in Ar atmosphere.

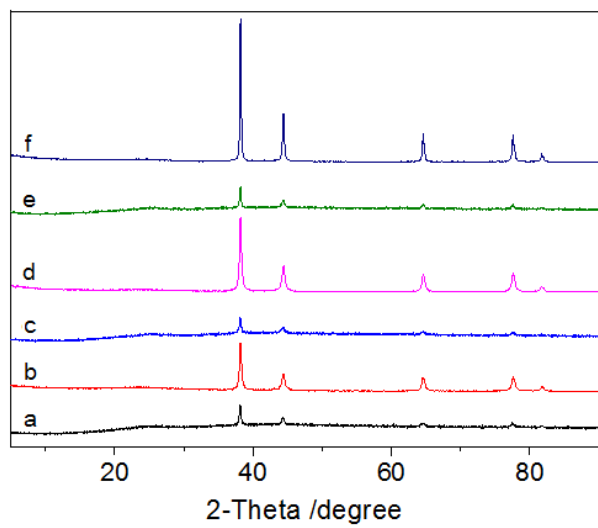


Fig. S7 XRD patterns of (a) AuCo/NXC-1, (b) Au/NXC-1, (c) AuCo/NXC-2, (d) Au/NXC-2, (e) AuCo/NXC-3 and (f) Au/NXC-3.

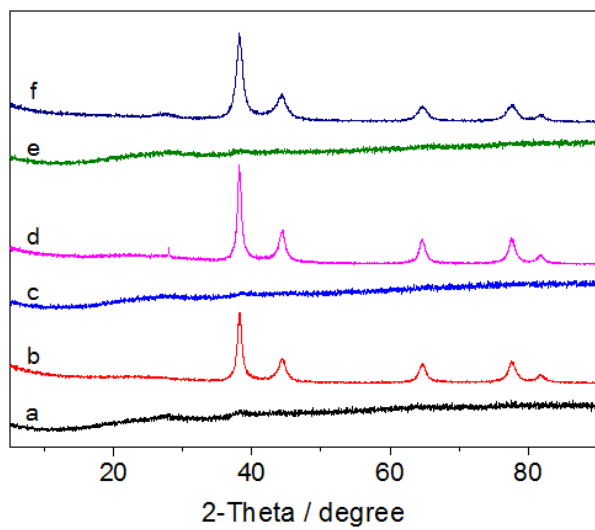


Fig. S8 XRD patterns of (a) AuCo/C₃N₄-1, (b) Au/C₃N₄-1, (c) AuCo/C₃N₄-2, (d) Au/C₃N₄-2, (e) AuCo/C₃N₄-3 and (f) Au/C₃N₄-3.

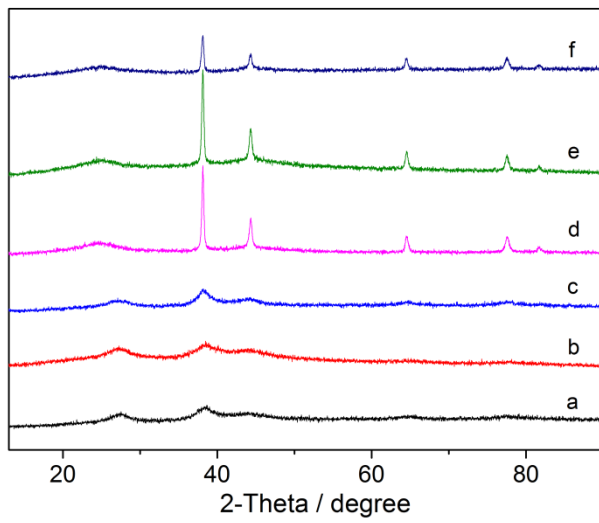


Fig. S9 XRD patterns of (a) AuNi/C₃N₄-1, (b) AuNi/C₃N₄-2, (c) AuNi/C₃N₄-3, (d) AuNi/NXC-1, (e) AuNi/NXC-2 and (f) AuNi/NXC-3.

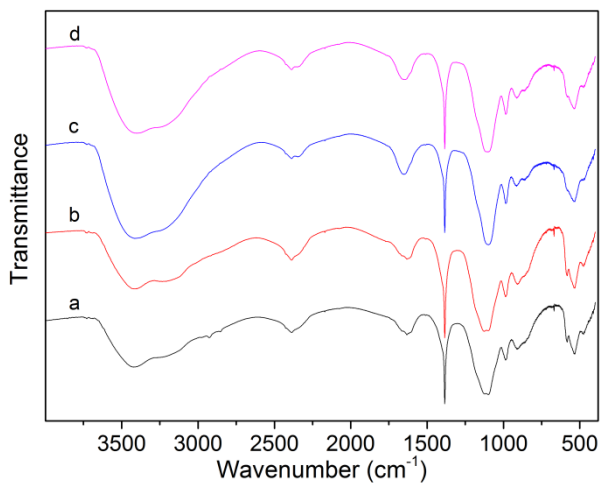


Fig. S10 IR spectra of (a) NXC, (b) AuCo/NXC-1, (c) AuCo/NXC-2 and (d) AuCo/NXC-3.

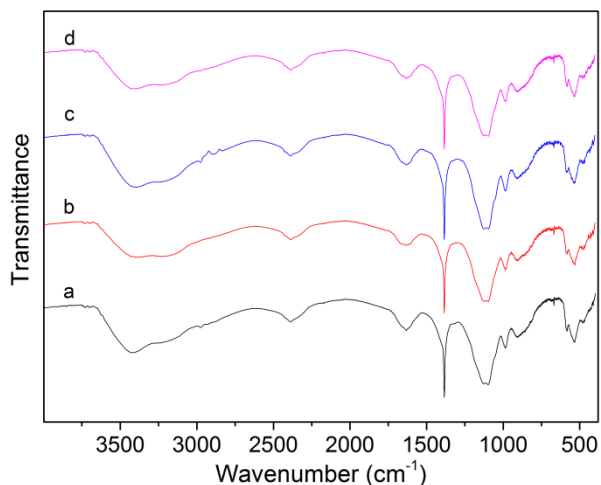


Fig. S11 IR spectra of (a) C_3N_4 , (b) AuCo/ C_3N_4 -1, (c) AuCo/ C_3N_4 -2 and (d) AuCo/ C_3N_4 -3.

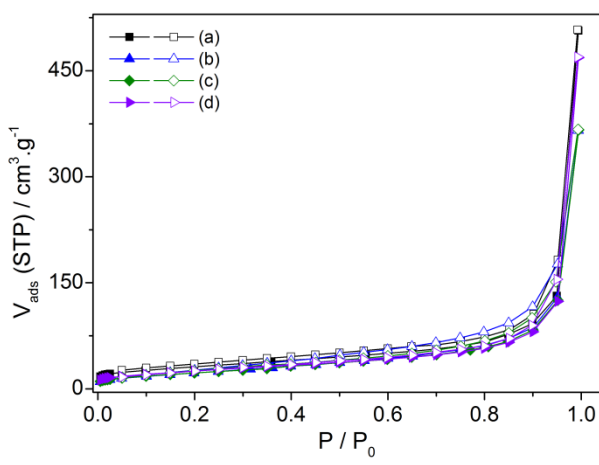


Fig. S12 N_2 sorption isotherms of (a) NXC, (b) AuCo/NXC-1, (c) AuCo/NXC-2 and (d) AuCo/NXC-3 (Au/Co = 1/7) at 77 K.

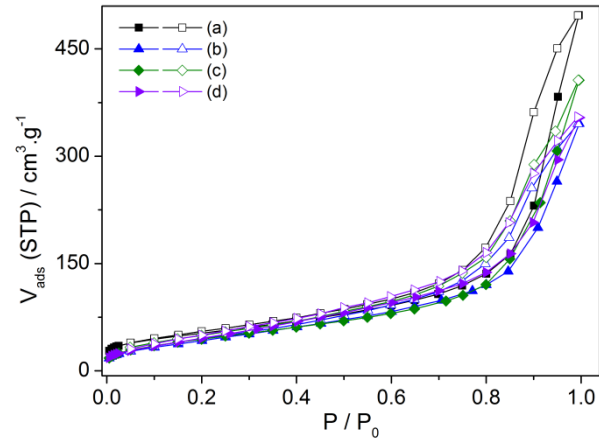


Fig. S13 N_2 sorption isotherms of (a) C_3N_4 , (b) AuCo/ C_3N_4 -1, (c) AuCo/ C_3N_4 -2 and (d) AuCo/ C_3N_4 -3 (Au/Co = 1/7) at 77 K.

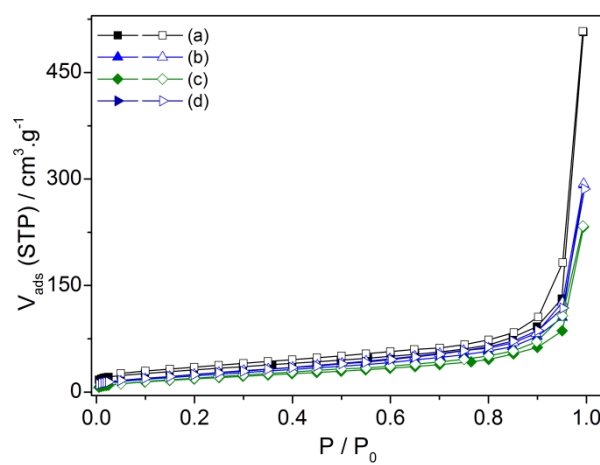


Fig. S14 N_2 sorption isotherms of (a) NXC, (b) AuNi/NXC-1, (c) AuNi/NXC-2 and (d) AuNi/NXC-3 ($\text{Au}/\text{Co} = 1/7$) at 77 K.

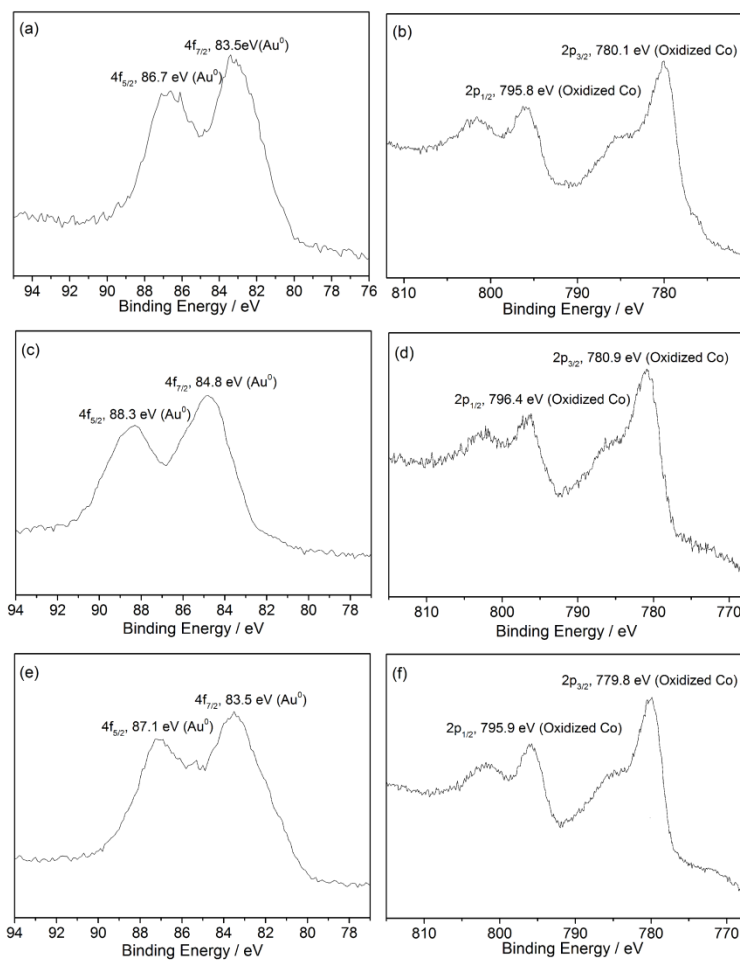


Fig. S15 XPS spectra for (a, b) AuCo/C₃N₄-1, (c, d) AuCo/C₃N₄-2 and (e, f) AuCo/C₃N₄-3 (Au/Co = 1/7).

Table S1 TOF and E_a values for hydrolysis of AB catalysed by different catalysts at 298 K.

Catalyst	TOF ($\text{mol}_{\text{H}_2} \cdot \text{mol}_{\text{cat}}^{-1} \cdot \text{min}^{-1}$)	Ref.
AuCo/NXC-1	42.1	This work
AuCo/NXC-2	7.2	This work
AuCo/NXC-3	12.6	This work
AuCo/C ₃ N ₄ -1	30.6	This work
AuCo/C ₃ N ₄ -2	6.4	This work
AuCo/C ₃ N ₄ -3	14.7	This work
AuCo/XC-1	31.6	This work
AuCo/XC-2	1.6	This work
AuCo/XC-3	7.2	This work
Au-Co@CN with light	48.28	10
Au-Co@CN	28.4	10
Pd@Co/graphene	40.9	9(d)
Ru@Co/graphene	40.46	7(o)
Co/PEI-GO	39.9	19(d)
In situ Co	39.8	19(a)
Co(0) nanoclusters	25.7	22(a)
AuCo@MIL-101	23.5	20
CuCo@MIL-101	19.6	9(e)
Cu@Co	15	7(h)
Au@Co	13.7	7(d)
Cu@FeCo	10.5	22(b)
Ag@Co/graphene	10.23	19(c)
Co/hydroxyapatite	4.54	24(b)
Co/Al ₂ O ₃	2.08	24(a)

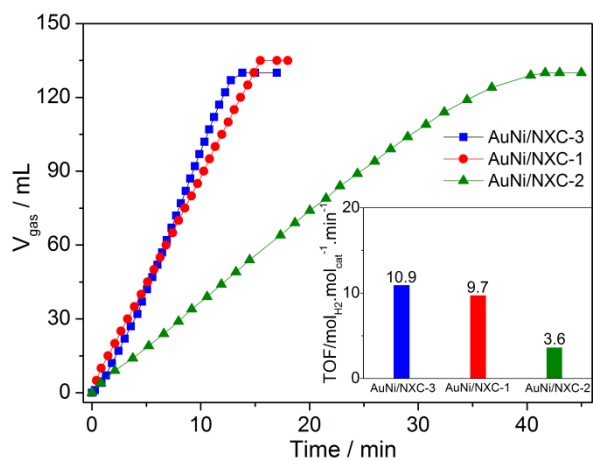


Fig. S16 Plots of time versus volume of H_2 generated from aqueous NH_3BH_3 (0.276 M, 6.2 mL) over AuNi/NXC-3, AuNi/NXC-1 and AuNi/NXC-2 at room temperature.

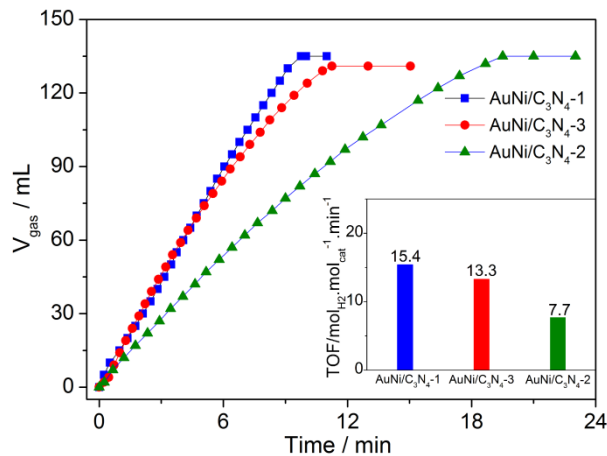


Fig. S17 Plots of time versus volume of H_2 generated from aqueous NH_3BH_3 (0.276 M, 6.2 mL) over AuNi/C₃N₄-1, AuNi/C₃N₄-3 and AuNi/C₃N₄-2 at room temperature.

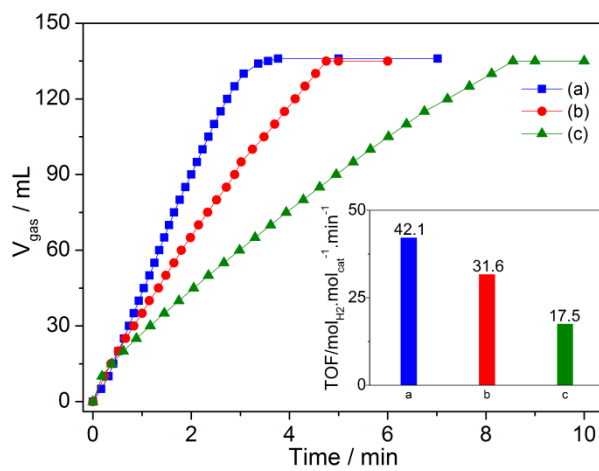


Fig. S18 Plots of time versus volume of H_2 generated from aqueous NH_3BH_3 (0.276 M, 6.2 mL) over $\text{AuCo}/\text{NXC-1}$ with different mole ratio of Au/Co : (a) 1:7; (b) 1:3; (c) 1:1.

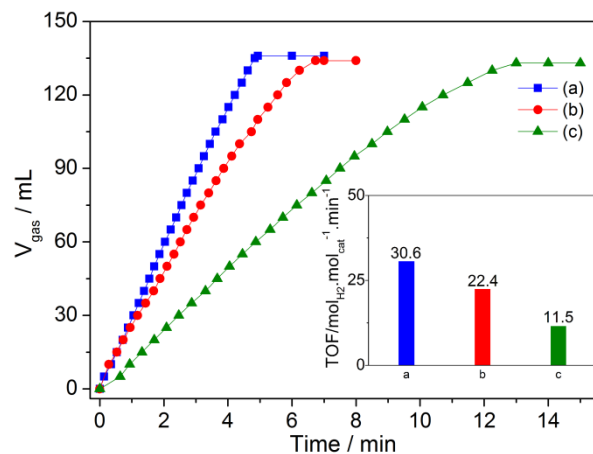


Fig. S19 Plots of time versus volume of H_2 generated from aqueous NH_3BH_3 (0.276 M, 6.2 mL) over $\text{AuCo}/\text{C}_3\text{N}_4\text{-1}$ with different mole ratio of Au/Co : (a) 1:7; (b) 1:3; (c) 1:1.

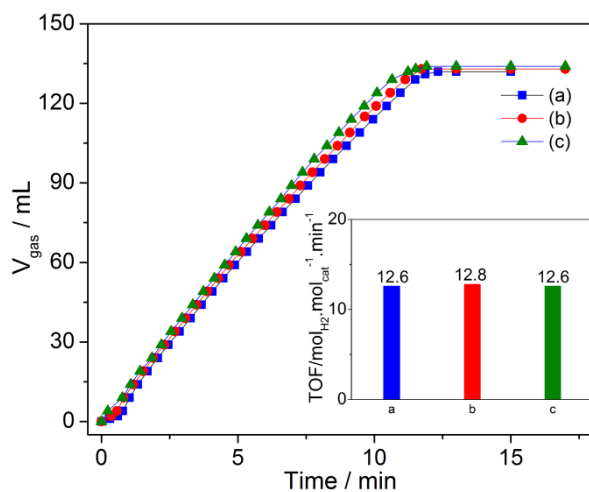


Fig. S20 plots of time versus volume of H_2 generated from aqueous NH_3BH_3 (0.276 M, 6.2 mL) over $\text{AuCo}/\text{NXC-3}$ with different mole ratio of Au/Co : (a) 1:7; (b) 1:3; (c) 1:1.

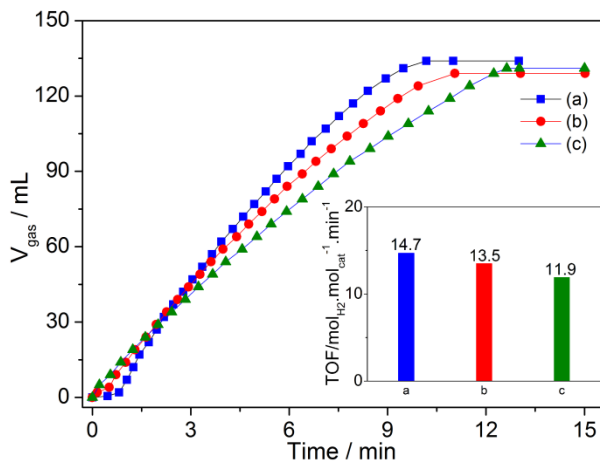


Fig. S21 plots of time versus volume of H_2 generated from aqueous NH_3BH_3 (0.276 M, 6.2 mL) over $\text{AuCo}/\text{C}_3\text{N}_4\text{-3}$ with different mole ratio of Au/Co : (a) 1:7; (b) 1:3; (c) 1:1.

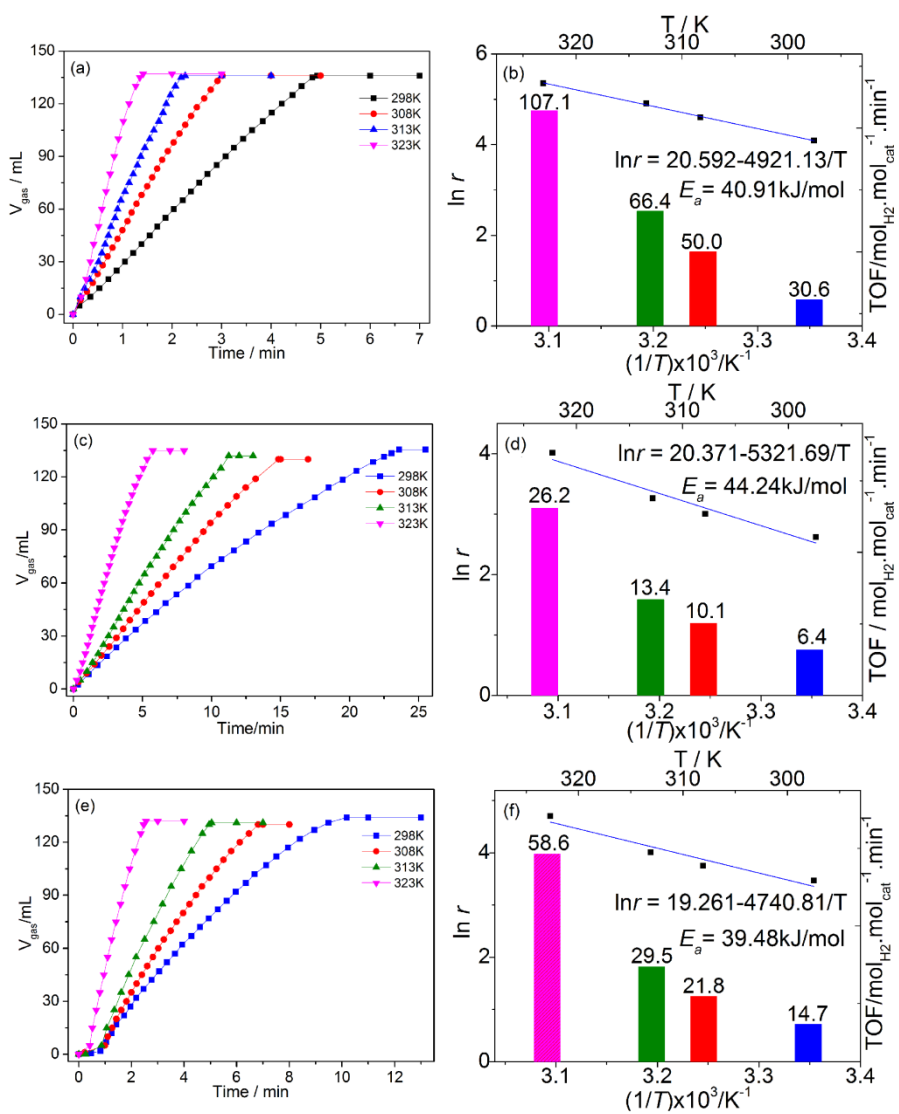


Fig. S22 Plots of time versus volume of H_2 generated from aqueous NH_3BH_3 (0.276 M, 6.2 mL) and Arrhenius plots and TOF values of NH_3BH_3 dehydrogenation over (a, b) AuCo/C₃N₄-1, (c, d) AuCo/C₃N₄-2, and (e, f) AuCo/C₃N₄-3 (Au/Co = 1/7) at different temperatures.